Research & Reviews: Journal of Pure and Applied Physics

Physical and Optical Analysis of Erbium Doped Magnesium Zinc Phosphate Glass

Sahar MR*, Zain SK, Ishak NA, Sazali ES and Yusoff NM
Faculty of Science, Department of Physics, Advanced Optical Materials Research Group, University Technology, Malaysia

Research Article

Received date: 23/10/2015
Accepted date: 01/12/2015
Published date: 12/03/2015

***For Correspondence**

Sahar MR, Faculty of Science, Department of Physics, Advanced Optical Materials Research Group, University Technology, 81310 UTM Skudai, Johor, Malaysia, Tel: +607-5566162

E-mail: mrahim057@gmail.com

Keywords: Phosphate glasses, XRD, Optical energy, Band gap, Bonding characteristic, Racah parameter

ABSTRACT

Glasses with composition of (60-*x*)P_2O_5-10MgO-30ZnO-(*x*)Er_2O_3 where x = 0, 0.5, 1.0 and 1.5 mol% have successfully been prepared by melt quenching technique. The amorphous nature of the glass has been determined by using X-ray Diffractometer (XRD). It is found that all glasses are amorphous in nature. The physical properties have been determined by mean of glass density and molar volume, while the optical properties have been characterized by UV-Vis Spectroscopy (UV-Vis). The glass density is found to be in range of (2.753-2.791) g cm^{-3} and is increasing as the Er_2O_3 concentration is increased up to 0.5 mol%, but decreases as the Er_2O_3 concentration is further increased up to 1.5 mol%. The molar volume of the glass exhibits an opposite trend with the density. UV-Vis spectra reveal seven absorption bands from the ground state $^4I_{15/2}$ to to the excited states $^4F_{7/2}$, $^2H_{11/2}$, $^4S_{3/2}$, $^4F_{9/2}$, $^4I_{9/2}$, $^4I_{11/2}$ and $^4I_{13/2}$, centered at 486, 520, 550, 650, 792, 974 and 1536 nm, respectively. The optical energy band gap of the glass decreases as the Er_2O_3 concentration is increased from 0.0 mol% to 0.5 mol% but increases as the Er_2O_3 concentration is further increased up to 1.5 mol%. Bonding characteristic of the glass is determined via calculation of Racah parameter. All the results are discussed with respect to the Er_2O_3 concentration.

INTRODUCTION

Recently, a lot of works are carried out into the study of phosphate glasses due to their good chemical and physical properties which is suitable for the application in the field of optical communication. Phosphate based glass has queried much attention due to their excellent properties such as high transparency, low melting point, high thermal stability, low dispersion and low refractive index [1]. Phosphate glass exhibits high solubility of rare earth ions which allowing high concentration of active ion without losing their peculiar properties [2-4].

The present of metal oxide in host material will improve the phosphate glass stability due to the P-O-M^+ (M is the metal cation) which is generally more stable to the atmospheric hydrolysis [5]. The addition of zinc and magnesium will affect the properties of glass in different way. According to the previous work, the presence of Zn^{2+} and Mg^{2+} will improve the polarizable and chemical durability of glass, respectively [6].

Besides, rare earth doped phosphate glass gives such of excellent improvement in the development of many optical devices [7]. It gives higher emission efficiency with the enhancement in emission line from visible to the infrared spectral region under suitable excitation condition as reported elsewhere [8]. Among the rare earth ions, Er^{3+} ion has higher potential application in developing the optical and laser device. The presence of Er^{3+} ion in phosphate glass can generate 1.54 *μm* wavelengths which can be utilized for optical amplification and its visible upconversion emission can be used as a solid-state laser [9].

The purpose of this study is to prepare (60-*x*)P_2O_5-10MgO-30ZnO-(*x*)Er_2O_3 glass system by melt quenching technique and characterize their physical and optical properties. There are some advantages of melt quenching technique, which is easier than other method and can produce flexible glass geometry. The results are analysed, compared to the previous research and understood.

EXPERIMENTAL

The raw material of P_2O_5, MgO, ZnO and Er_2O_3 are commercially provided in the powder forms. 20 gm batch from a proportion amount of P_2O_5 (purity 99.9%), MgO (purity 99.5%), ZnO (purity 99.1%) and Er_2O_3 (purity 99.9%) powder are weighed and mixed in an alumina crucible before being heated at 900°C for 30 minutes. After the required viscosity is obtained, the melts is quenched in a pre-heated metal plates. The glass is then annealed at 300°C for 3 hours before being allowed to cool down to room temperature. The composition for each sample of the glass is shown in **Table 1.**

Table 1. The Nominal Composition of Glass Samples.

Sample	Concentration (mol %)			
	P_2O_5	MgO	ZnO	Er_2O_3
S1	60.0	10.0	30.0	0.0
S2	59.5	10.0	30.0	0.5
S3	59.0	10.0	30.0	1.0
S4	58.5	10.0	30.0	1.5

X-ray Diffraction (XRD) analysis is performed by using Siemens Diffractometer D5000 using Cu-Kα radiations (λ≈1.54 Å) at 40 kV and 100 mA, with scanning angle of 2θ ranges between 10-80°. The glass density (ρ in gcm^{-3}) is determined by using the Archimedes method with toluene is used as an immersion liquid. The relation of Archimedes principle is written as [10],

$$\rho = \frac{W_a}{W_a - W_l}(\rho_l - \rho_a) + \rho_a \quad (1)$$

where W_a and W_l are the weight of glass in air and in liquid, respectively. ρ_a is the air density (0.001 g cm^{-3}) and ρ_l is the density of toluene (0.8669 g cm^{-3}). Meanwhile, the molar volume, V_m is calculated by using the relation [11]:

$$V_m = (\frac{M}{\rho}) \quad (2)$$

where *M* is the molar mass of glass.

The absorption spectra have been performed in the range of 400-1600 nm by using the Shimadzu 3101 UV-Vis spectrophotometer. Optical absorption reflects to the density of states at the band edges which is used to calculate the glass absorption coefficient α(*v*) using Beer Lambert's law as stated below [12],

$$\alpha(\nu) = 2.303\frac{A}{d} \quad (3)$$

where *A* is defined by log (I_o/I).

The absorption coefficient, α is used to calculate the optical energy band gap (E_g) using Davis Mott equation [13];

$$\alpha(\omega)\,\hbar\omega = C\,(\hbar\omega - Eg)^m \quad (4)$$

where $\hbar\omega$ is the photon energy, *C* is a constant, *α* absorption coefficients, *ω* is a frequency dependent and *m* is the index value.

Racah parameter is useful to interpret the electrostatic repulsion in an atom when more than one electron exists. The total repulsion can be determined in terms of B and C Racah parameter [14]. The symbol of B and C represents a complex form from a transition metal in the free ion. The nephelauxetic ratio, h is used to elucidate the effect of reduction or enhancement electron-electron repulsion between RE and ligand. The nephelauxetic ratio is a parameter used to explain the electron cloud expanding as early defined by Jorgensen [15]. All these parameters are calculated from absorption peak wavelength marked as (v_1, v_2, v_3 in cm^{-1}), which finally provide the information of ionic or covalent between metal and ligand bond. The amorphous field strength (*Dq*) and the Racah Parameter *B, C* can be calculated from the following relations [16],

$$v_1 = 10Dq \quad (5)$$

$$B = 1/3\,(2v_1 - v_2)(v_2 - v_1)\,/9v_1 - 5v_2 \quad (6)$$

$$C = v_3 - 4B - 10Dq/3 \quad (7)$$

The bonding formation can be predicted as:

$$h = [(B_{free} - B)/B_{free}]\,k_{ion} \quad (8)$$

$$k_{ion} = [Z + 2 - S/5]^2 \quad (9)$$

RESULTS AND DISCUSSION

Figure 1 shows the typical XRD pattern for all samples which shows the presence of broad hump in the range of 20-30 degree. The broad peak confirmed the amorphous nature of the glass sample.

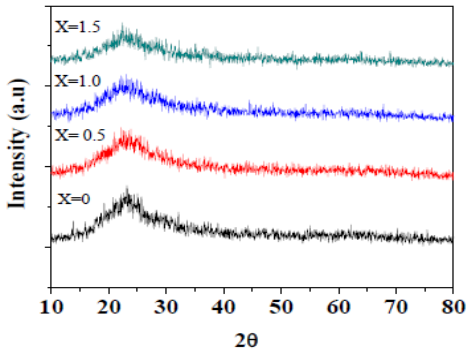

Figure 1. X-Ray Diffraction pattern of (60-*x*)P_2O_5-10MgO-30ZnO-(*x*)Er_2O_3 glass system.

The density and molar volume of the glasses are listed in **Table 2.** The relation of glass density and molar volume with the Er^{3+} concentration is shown in **Figure 2.** Glass density is found to be in the range of 2.754 - 2.915 g cm^{-3}. The glass densiy increases with the concentration of Er^{3+} ions up to 1.0 mol%, but decreases as the Er^{3+} concentration is increased up to 1.5 mol%. The addition of Er^{3+} into the glass network increases the number of non-bridging oxygen (NBO) and it also attributes to the replacement of atom with low density oxide (P_2O_5, 2.39 g cm^{-3}) with the atom of high density oxide (Er_2O_3, 8.64 g cm^{-3}) [4]. However, at the same range of Er^{3+} concentration, the molar volume shows an opposite behavior to the density where it decreases from 41.257 to 40.594 cm^3 mol^{-1} which presumably due to the decreases in the bond length or inter-atomic spacing between the atom. It is known that, the density and molar volume of material show an opposite behavior to each other [17].

Table 2. The Density and Molar Volume of (60-x)P_2O_5-10MgO-30ZnO-(x)Er_2O_3 Glasses.

Er_2O_3 concentration (mol%)	Density, ρ (±0.001)(g cm^{-3})	Molar Volume, V_m (±0.001)(cm^3 mol^{-1})
0.0	2.754	41.257
0.5	2.802	40.594
1.0	2.915	40.792
1.5	2.788	40.896

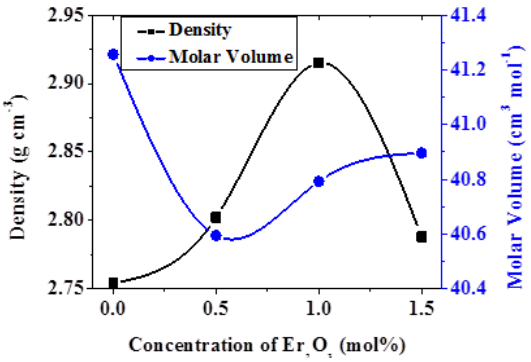

Figure 2. The density and molar volume of (60-x)P_2O_5-10MgO-30ZnO-(x)Er_2O_3 glass system dependent concentration of Er_2O_3.

As the Er^{3+} is increases beyond 0.5 mol% it is presumed that the Er^{3+} ion will enter the network by breaking up the phosphate double bond. As a consequent, there will be a relatively increase in the amount of bridging oxygen (BO). This result shows the role of Er^{3+} in modifying the glass structure from PO_3 to PO_4. On the other hand, the increases of BO network will cause the increase in bond length or inter-atomic spacing between the atom and thus gives the increase in molar volume of the glass.

Figure 3a shows the optical absorption spectra of the glass. Basically, the appearance peak in the spectra is due to the distribution of crystal field in the glass. From **Figure 3a**, it shows seven absorption peaks which correspond to the transition of Er^{3+} from ground state $^4I_{15/2}$ to the excited states of $^4F_{7/2}$, $^2H_{11/2}$, $^4S_{3/2}$, $^4F_{9/2}$, $^4I_{9/2}$, $^4I_{11/2}$ and $^4I_{13/2}$ centered at 486, 520, 550, 650, 792, 974 and 1536 nm, respectively.

From **Figure 3a**, a plot of $(\alpha hv)^{1/2}$ against photon energy(hv) can be made and the result is shown in **Figure 3b.** From **Figure 3b**, the values of E_g can be estimated by extrapolating a linear part of $(\alpha hv)^{1/2}$ against photon energy(hv). The meeting point of the straight line and x-axis is the value of the E_g of the sample. The value of E_g is summarized in **Table 3.** It can be seen that the value is in the range of (4.236 – 3.698) eV which is close to the result obtained in the previous work [18].

As can be seen that E_g decreases as the amount of Er^{3+} concentration is increased up to 0.5 mol%, but slightly increases as further Er^{3+} is increased up to 1.5 mol%. The decrease of E_g is probably due to the increasing number of non-bridging oxygen

(NBO) [19]. However further addition of the Er^{3+} ion shows an increasing of the E_g which indicates the increase in the formation of bridging oxygen (BO) in the glass. The larger magnitude of BO's, more energy is needed to excite the electrons to the upper state. This is due to the fact that the electrons are tightly bounded to the BO as compare to the electron connected to NBO. This changes is parallel to the results as observed in the variation of density.

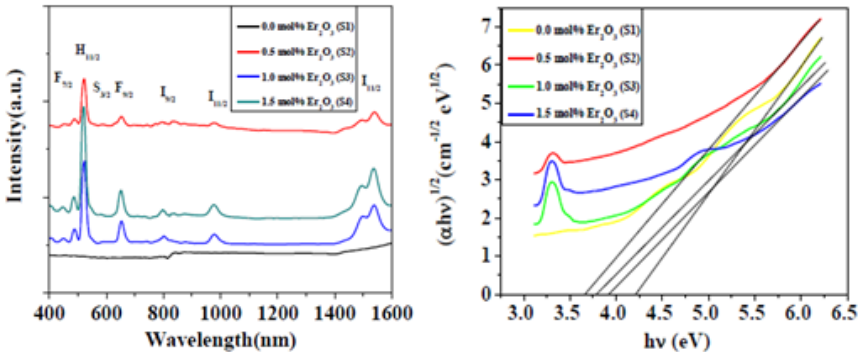

Figure 3. (a) The optical absorption spectra (b) The $(\alpha hv)^{1/2}$ against photon energy (hv) of $(60\text{-}x)P_2O_5$-10MgO-30ZnO-$(x)Er_2O_3$ glasses.

Table 3. The Optical Energy Band gap (E_g) for the Prepared Glasses.

Sample	Er_2O_3 concentration (mol%)	E_g (±0.001 eV)
S1	0.0	4.236
S2	0.5	3.698
S3	1.0	3.800
S4	1.5	3.910

From **Figure 4a**, it can be seen that parameter B is increasing as Er_2O_3 is increased up to 1.0 mol% Er_2O_3. The increasing of parameter B shows that Er–O bond is ionic. However, as the Er_2O_3 is further increased, the B parameter decreases which reflects to the increase in covalent bond between Er^{3+} ion and ligand. It indicates that more electrons delocalized in the d-shell as reported elsewhere [20]. From **Figure 4b**, it can be seen that parameter C shows a similar trend as parameter B but keep increasing beyond 1.0 mol%. This increment is presumably due to the mix between ionic with covalence bond of Er-O. **Figure 5a** shows the ratio of crystal field Dq to parameter B against the Er_2O_3 concentration.

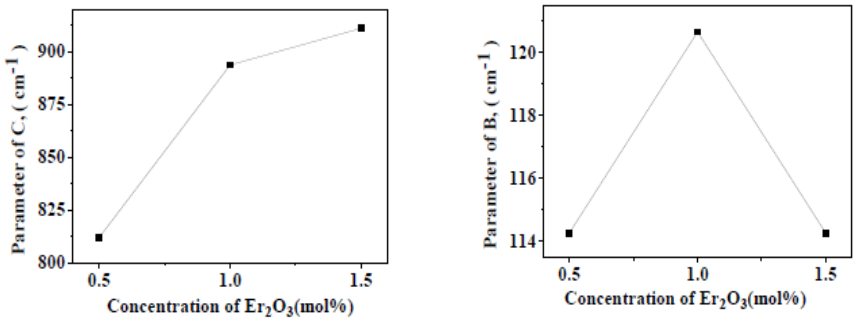

Figure 4. (a) Parameter B (b) Parameter C versus Er_2O_3 concentration in mol%.

From **Figure 5a**, it can be seen that the ratio of Dq/B decreases as increasing of Er_2O_3 concentration. The reduction of Dq/B from 16.830 to 13.300 reflected that the bond of Er-O has smaller crystal field strength. Meanwhile, the nephelauxetic function is decreasing from 0.061 to 0.059 with the addition of Er_2O_3 concentration up to 1.0 mol% as shown in **Figure 5b**. This is once again shows that the Er-O bonds are ionic because of the less overlapping of d-orbital of Er^{3+} and ligand orbital. Beyond 1.0 mol%, the Nephelauxetic function increases with Er_2O_3 concentration. This is due to the increasing of overlapping in Er-O orbital [21,22].

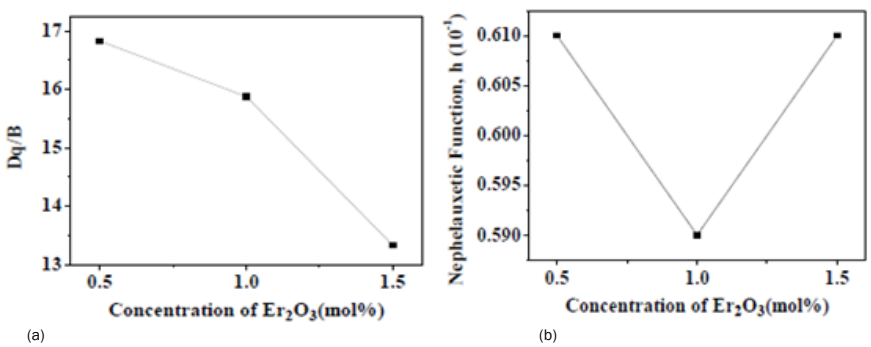

Figure 5. (a) Dq/B (b) Nephelauxetic Function, h versus Er_2O_3 concentration in mol%.

CONCLUSION

A series of glass with composition of (60-*x*)P_2O_5-10MgO-30ZnO-(*x*)Er_2O_3 where x = 0, 0.5, 1.0, and 1.5 mol% have successfully been prepared by melt quenching technique. All glasses are found amorphous in nature. The glass density is found in the range of (2.754 - 2.915) g cm^{-3}, increases with the increasing of Er^{3+} concentration up to 1.0 mol%, but decreases as the concentration of Er^{3+} is added up to 1.5 mol%. The molar volume of the glass is found to be in the range of (41.257 - 40.594) cm^3 mol^{-1}. The variation of density and molar volume of the glass is due to the rearrangement of the lattice cause by the increasing number of non-bridging oxygen (NBO) and bridging oxygen (BO). The UV-Vis spectra reveal seven absorption bands centered at 486, 520, 550, 650, 792, 974 and 1536 nm which correspond to the transition of Er^{3+} from ground state to excited state $^4I_{15/2}$ to the excited states of $^4F_{7/2}$, $^2H_{11/2}$, $^4S_{3/2}$, $^4F_{9/2}$, $^4I_{9/2}$, $^4I_{11/2}$ and $^4I_{13/2}$ respectively. The optical energy band gap (E_g) is found to decrease as the Er^{3+} concentration is increased from 0.0 mol% to 0.5 mol%, but increases as the Er^{3+} concentration is further increased up to 1.5 mol%. Racah parameter B and C are found to be in the range of (114.262-120.667) cm^{-1} and (812.025-893.890) cm^{-1}, respectively. Meanwhile the *Dq/B* and h are (16.830-13.300) and (0.061-0.059), respectively. The bonding parameters are depending on the composition of Er_2O_3. It is found that the Er-O bond becomes more covalence as Er_2O_3 is increased.

ACKNOWLEDGEMENTS

The authors gratefully acknowledge the financial support from Ministry of Education, Malaysia and Universiti Teknologi Malaysia via grants of Vot: 05H45, 05H36, 4F424, 4F319, 4F083, and 07J80.

REFERENCES

1. Suratwala TI et al. Effects of OH content, water vapor pressure, and temperature on sub-critical crack growth in phosphate glass. Journal of Non-Crystalline Solids 2000; 213-227
2. Jiang S et al. Er^{3+}-doped phosphate glasses for fiber amplifiers with high gain per unit length. Journal of Non-Crystalline Solid 2000; 263, 364-368.
3. Narayanan MK and Shashikala HD. Optimization of melt-quenching process parameters for refractive index of barium phosphate glasses using Taguchi method. Procedia Materials Science. 2014; 5: 304-306.
4. Aboulfotoh N et al. Charaterization of copper doped phosphate glasses for optical applications. Ceramic International. 2014; 40: 10395-10399.
5. Bae BS and Weinberg MC. Oxidation-reduction equilibrium in copper phosphate-glass melted in air. Journal Amorphous Ceramic. 1991; 74: 3039-3045.
6. Smith CE and Brow RK. The Properties and Structure of Zinc Magnesium phosphate glasses. Journal of Non-Crytalline Solid. 2014; 390: 51-58.
7. Nogami M et al. Site-dependent fluorescence and hole-burning spectra of Eu^{3+}-doped Al_2O_3–SiO_2 glasses. Journal of Luminescence. 2000; 117-123.
8. Parchur K et al. Observation of intermediate bands in Eu^{3+} doped YPO_4 host: Li^+ ion effect and blue to pink light emitter. AIP Advances. 2012; 2: 032119.
9. Mazurak Z et al. Optical properties of Pr, Sm, and Er doped P_2O_5-CaO-SrO-BaO phosphate glass. Optical Material. 2010; 547-553.
10. Shelby JE. Introduction to Glass Science and Technology. 2nd. ed. London: Royal Society of Chemistry. 2005
11. El-Diasty F and Wahab AA. Optical Band Gap Studies on Lithium Aluminum Silicate Glasses doped with Cr^{3+} ions. Journal of Applied Physics. 2006; 100: 093511-1-7
12. Knowles A and Burgess C. Practical Absorption Spectrometry. New York: Chapman and Hall. 1984
13. Sazali ES et al. Optical properties of gold nanoparticle embedded Er^{3+} doped lead–tellurite glasses. Journal of Alloys and Compounds. 2014; 607: 85-90.
14. Hassan MA et al. ESR and ligand field theory studies of Nd_2O_3 doped borochromate glasses. Journal of Alloys and Compounds. 2012; 539: 233-236
15. Jorgensen CK. Modern Aspect of Ligand field Theory. Amsterdam: North-Holland Publishing Co. 1971.
16. Dayanand C et al. IR and Optical propertiees of PbO glasss containing a small amount of silica. Material Letters. 1995; 23: 309-315.
17. Chanshetti UB et al. Density and molar volume of phosphate glasses. Physics, Chemistry and Technology. 2011; 9: 29-36.
18. Anigrahawati P et al. Influence of Fe_3O_4 nanoparticles on structural, optical and magnetic properties of erbium doped zinc phosphate glass. Materials Chemistry and Physics. 2015; 155: 155-161.

19. El-Batal AH et al. Gamma rays interaction with copper doped lithium phosphate glasses. Journal of Molecular Structure. 2013; 1054-1055: 57-64.

20. Kesavulu CR et al. EPR, Optical Absorption and Photoluminescence Properties of Cr^{3+} ions in Lithium Borophosphate Glasses. Journal of Alloys and Compounds. 2010; 496: 75-80

21. Ravikumar RVSSN et al. EPR and Optical studies on Transition Metal doped $LiRbB_4O_7$ Glasses. Journal of Physics and Chemistry of Solids. 2003; 64: 261

22. Giridhar G et al. Spectroscopic Studies on Pb_3O_4–ZnO–P_2O_5 Glasses doped with Transition Metal Ions. Physica B. 2011; 406: 4027